Article

Journal of Vibration and Control
2018, Vol. 24(21) 4933–4944

DOI: 10.1177/1077546317739794
journals.sagepub.com/home/jvc
SAGE

Acoustic metamaterials with combined heterogeneous double-split hollow sphere for noise reduction

Jung Sik Choi and Gil Ho Yoon

Abstract

We present the concept design of a new class of acoustic metamaterial structure based on a combined heterogeneous double-split hollow sphere (CHDSHS). These structures are local resonators possessing subwavelength band gaps. The present CHDSHS metamaterial structures are made of plastic sphere structures with two different holes. The main novelty of a CHDSHS relies in the significant noise reduction obtained and the simplicity of manufacture. Their characteristics in band gaps are influenced by the volume sizes of the plastic sphere and the areas of the two holes. The CHDSHS metamaterials are combined to increase pressure attenuation over a wide frequency range. The frequency shifts in the band gap due to the changes in size are formulated and discussed in detail. Furthermore, the band gaps of the present CHDSHS metamaterials are numerically and experimentally demonstrated.

Keywords

Acoustic metamaterial structure, double-split hollow sphere, combined heterogeneous double-split hollow sphere, resonator, noise reduction

1. Introduction

A new type of acoustic metamaterial structure with various sized holes is developed for a wide stop band, i.e., frequency zones with no free wave propagation over a certain frequency range of interest; its performance is theoretically studied and experimentally tested in this study. Of Bragg-scattering-based interference and resonance-based-interference, the metamaterial mechanism presented here is based on resonance-based interference. As the sizes of the present metamaterials are relatively small, the presented structure can be installed in any place required. The acoustic wave propagation can be easily prevented in some designed frequency gaps in the presented acoustic metamaterial.

Metamaterials are artificial repeating composite materials or structures with desired unusual properties that are not found in nature (Kshetrimayum, 2004). First of all, metamaterials have been extensively studied in electromagnetics (Pendry, 2000; Smith et al., 2004; Shalaev et al., 2005). Electromagnetic metamaterials with a negative effective permittivity or a negative effective permeability have achieved significant success in theoretical studies and engineering research (Smith et al., 2004; Liu et al., 2008; Zhu et al., 2008). From a mathematical point of view, electromagnetic waves and acoustic waves share similarities in their governing equation, i.e., the Helmholtz equation. Therefore, acoustic metamaterials have also received great attention (Kushwaha et al., 1993; Liu et al., 2000; Li and Chan, 2004; Fang et al., 2006; Cummer and Schurig, 2007); some criticism also exists, as some acoustic metamaterial structures are simply repeating acoustic resonators. The band gaps of electromagnetic or acoustic metamaterials can be explained by Bragg scattering or local resonance (Liu et al., 2008; Zhu et al., 2008). Bragg scattering of waves is observed over the frequency range where the lattice constant of the material is less than half the wavelength of the scattered wave. Local resonances are observed in some

School of Mechanical Engineering, Hanyang University, Republic of Korea

Received: 16 January 2017; accepted: 26 September 2017

Corresponding author:
Gil Ho Yoon, School of Mechanical Engineering, Hanyang University, Seoul, Republic of Korea.
Emails: ghy@hanyang.ac.kr; gilho.yoon@gmail.com

frequency ranges when waves match the natural frequency of an object attached to the main structure. These resonances occur in acoustic metamaterials and are employed to manipulate propagating waves with wavelengths much larger than the resonant structures. The presented acoustic metamaterials are based on local resonances.

Many special acoustic structures or materials have been proposed to achieve these interesting negative material properties. For local-resonance acoustic metamaterials, monopolar or dipolar resonances show a negative bulk modulus or a negative mass density (Ding et al., 2007; Cheng et al., 2008; Huang and Sun, 2009; Huang et al., 2009; Lee et al., 2009). Furthermore, owing to the easy installation and manufacturing, local-resonance acoustic metamaterials have been successfully exploited for noise vibration control, lensing, and localization (Pennec et al., 2004; Ambati et al., 2007; Torrent and Sánchez-Dehesa, 2008; Li et al., 2009; Zhang et al., 2009; Zhu et al., 2010; Chiang et al., 2011; Lee et al., 2011; Popa et al., 2011). Liu et al. (2000) proposed the use of sonic crystals with tube-coated lead balls to produce negative effective elastic constants. Guo and Sheng (2016) proposed a periodic bi-layer beam structure with four components. Reynolds and Daley (2017) introduced an active metamaterial structure to control the bandgap. By introducing repeated shunted Helmholtz resonators, acoustic metamaterials with negative effective bulk modulus near the local resonant frequency were designed. To yield negative effective mass density, a class of acoustic metamaterial with tensioned membranes has been developed (Yang et al., 2008; Wang et al., 2008; Li et al., 2013; Chen et al., 2014a, 2014b).

Most acoustic metamaterials based on local resonance can be characterized by a passive response and have a limitation, as they operate at fixed narrow frequency ranges. To enhance the functionalities of acoustic metamaterials, several attempts have been made to adjust the local resonant band gaps or the Bragg scattering. Several authors (Cervera et al., 2002; Sheng et al., 2003; Wang et al., 2004; Liu et al., 2005; Fokin et al., 2007) have used instability-induced pattern deformation in polymers to modify the stiffness of the polymer structure and cause consequent changes in the band gap. A number of authors (Zhang et al., 2007; Airoldi and Ruzzene, 2011; Casadei et al., 2012; Chen et al., 2014c) utilized shunted piezoelectric materials to manipulate the characteristics of the stop band. In some work (Mead, 1970; Hirsekorn, 2004; Yao et al., 2008; Chen et al., 2011), the adaptive connectivity mechanism is utilized. Ding et al. (2013) demonstrated that by adjusting the relative positions of multiple holes of a double-split hollow sphere (DSHS), as shown in Figure 1(b), the local-resonance bandgap can be adjusted. Furthermore, unlike Helmholtz's resonator, the DSHS structures can be installed in a sealed plate; with the help of the holes of the DSHS structure, movement of fluid media through the plate is possible.

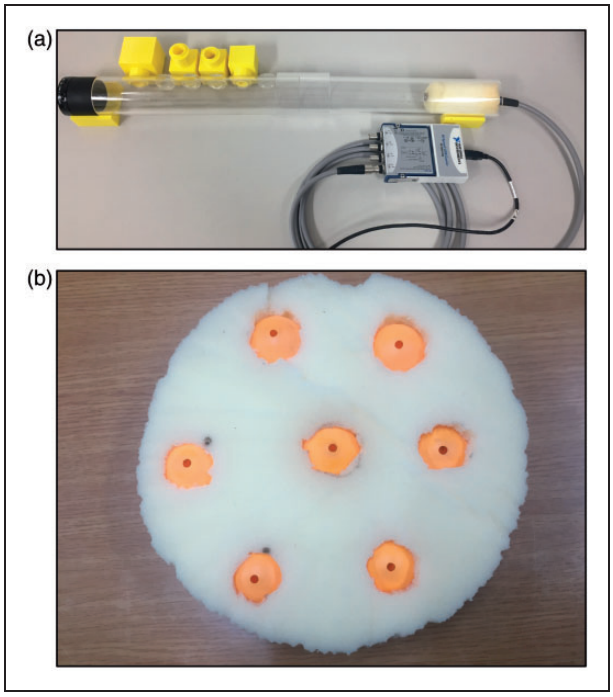

Figure 1. Acoustic metamaterial example: (a) acoustic duct and periodic Helmholtz resonators; (b) acoustic duct and double-split hollow sphere. (The foam is not used in this study and the acoustic metamaterials are not fixed in the experiment.)

This study investigates the characteristics of the DSHS acoustic metamaterial shown in Figure 1 and proposes a method to make a wideband acoustic metamaterial by making a DSHS array termed a combined heterogeneous double-split hollow sphere (CHDSHS) structure. A key idea of the present CHDSHS structure is that several heterogeneous double-split hollow sphere (HDSHS) structure acoustic metamaterials with different holes are used to make an array and the mutual coupling between several HDSHS acoustic metamaterials enables the creation of a wide stop band and significant noise reduction. The paper is organized as follows: Section 2 presents a study of the DSHS acoustic metamaterial. To achieve a wide stop band, the CHDSHS metamaterials are presented in Section 3. Our conclusions and future topics are summarized in Section 4.

2. Acoustic metamaterial with double-split hollow sphere

Figure 2 shows an acoustic metamaterial based on a DSHS. Ding et al. (2013) analyzed the characteristics

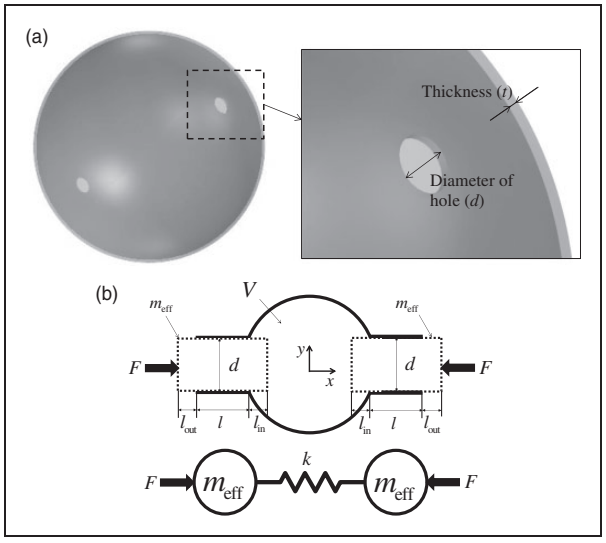

Figure 2. DSHS modeling: (a) 3D sphere with two holes; (b) equivalent spring–mass system.

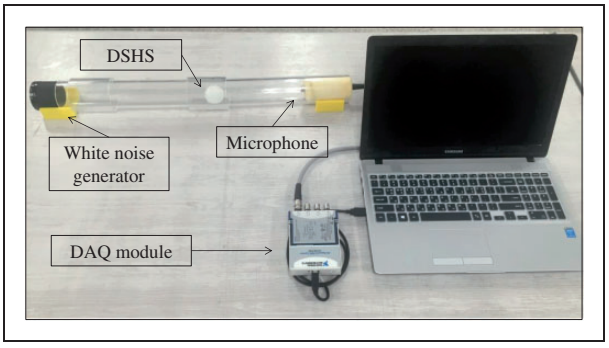

Figure 3. Experimental setup to measure the transmission of the double-split hollow sphere (DSHS) acoustic metamaterial. DAQ: data acquisition.

of the DSHS structures from an electromagnetic point of view, using an inductor–capacitor system. In this study, the characteristics of the DSHS structures are investigated from a mechanical engineering point of view, using a mass–spring system. Through this analytical method, we can derive a new characteristic equation. Unlike the Helmholtz resonator, with one mass and one spring, the DSHS structure has two masses and one spring. The acoustic mass comes from the effective acoustic masses at the small holes and the effective acoustic spring is realized through the cavity air. When the wavelength of the incident wave is much larger than the cross-sectional area of the DSHS resonator, the incident wave can be considered as a one-dimensional plane wave. It is possible to derive the transmission coefficient and the effective bulk modulus of this structured acoustic metamaterial. Also note that, owing to the two side holes, fluid can move back and forth inside the DSHS acoustic metamaterial.

The actual DSHS system cannot be moved by the vibrating acoustic forces. When the geometrical dimensions of the DSHS are much smaller than the wavelength, the DSHS resonator can be considered as an acoustic system with effective acoustic mass m_{eff} and effective acoustic spring constant k_{eff}, as (Kinsler et al., 1999; Blackstock, 2000)

$$m_{\text{eff}} = \rho_0 S L_{\text{eff}}, \quad k_{\text{eff}} = \rho_0 c^2 S^2 / V, \quad L_{\text{eff}} = L_0 + 1.4d/2 \tag{1}$$

where ρ_0 and c are the density of the medium and the speed of sound. The neck area, the effective height of the necks, the actual height of the necks, the diameter of the necks, and the cavity volume are denoted S, L_{eff}, L, d, and V, respectively. The governing equations of the DSHS can be formulated as

$$\begin{aligned} \text{Time domain}: & \; m_{\text{eff}}\ddot{x}_1^t = k_{\text{eff}}(x_2 - x_1), \; m_{\text{eff}}\ddot{x}_2^t \\ & = -k_{\text{eff}}(x_2 - x_1) \\ \text{Frequency domain}: & -\omega^2 m_{\text{eff}} x_1 = k_{\text{eff}}(x_2 - x_1), \\ & -\omega^2 m_{\text{eff}} x_2 = -k_{\text{eff}}(x_2 - x_1) \end{aligned} \tag{2}$$

$$\det\left(\begin{vmatrix} (k_{\text{eff}} - \omega^2 m_{\text{eff}}) & -k_{\text{eff}} \\ -k_{\text{eff}} & (k_{\text{eff}} - \omega^2 m_{\text{eff}}) \end{vmatrix}\right) = 0 \tag{3}$$

$$\begin{aligned} \omega_{\text{resonance}} &= \sqrt{\frac{2k_{\text{eff}}}{m_{\text{eff}}}} = \sqrt{\frac{2S}{L_{\text{eff}}V}}, \\ f_{\text{resonance}} &= \frac{c}{2\pi}\sqrt{\frac{2k_{\text{eff}}}{m_{\text{eff}}}} = \frac{c}{2\pi}\sqrt{\frac{2S}{L_{\text{eff}}V}} \end{aligned} \tag{4}$$

To verify the functions of DSHS experimentally, the experimental setup in Figure 3 was prepared. The air duct was made of a thick cylinder (diameter, 50 mm; length, 600 mm) and the DSHS structures were placed in the middle of the air duct. A white noise generator and a microphone were installed at the two sides and data acquisition equipment (NI-9234) was used for the measurement.

Figure 4 shows transmission curves for different hole sizes of the DSHS structures. It can be seen from Figure 4 that the pressure transmission is decreased at about 560 Hz, 720 Hz, 850 Hz, and 990 Hz for each DSHS structures and that these values are close to the theoretical values of about 563 Hz, 722 Hz, 855 Hz, and 971 Hz, respectively. With this DSHS structure, noise levels are reduced by about 120 dB, which is hard to achieve. Figure 5(b) shows the

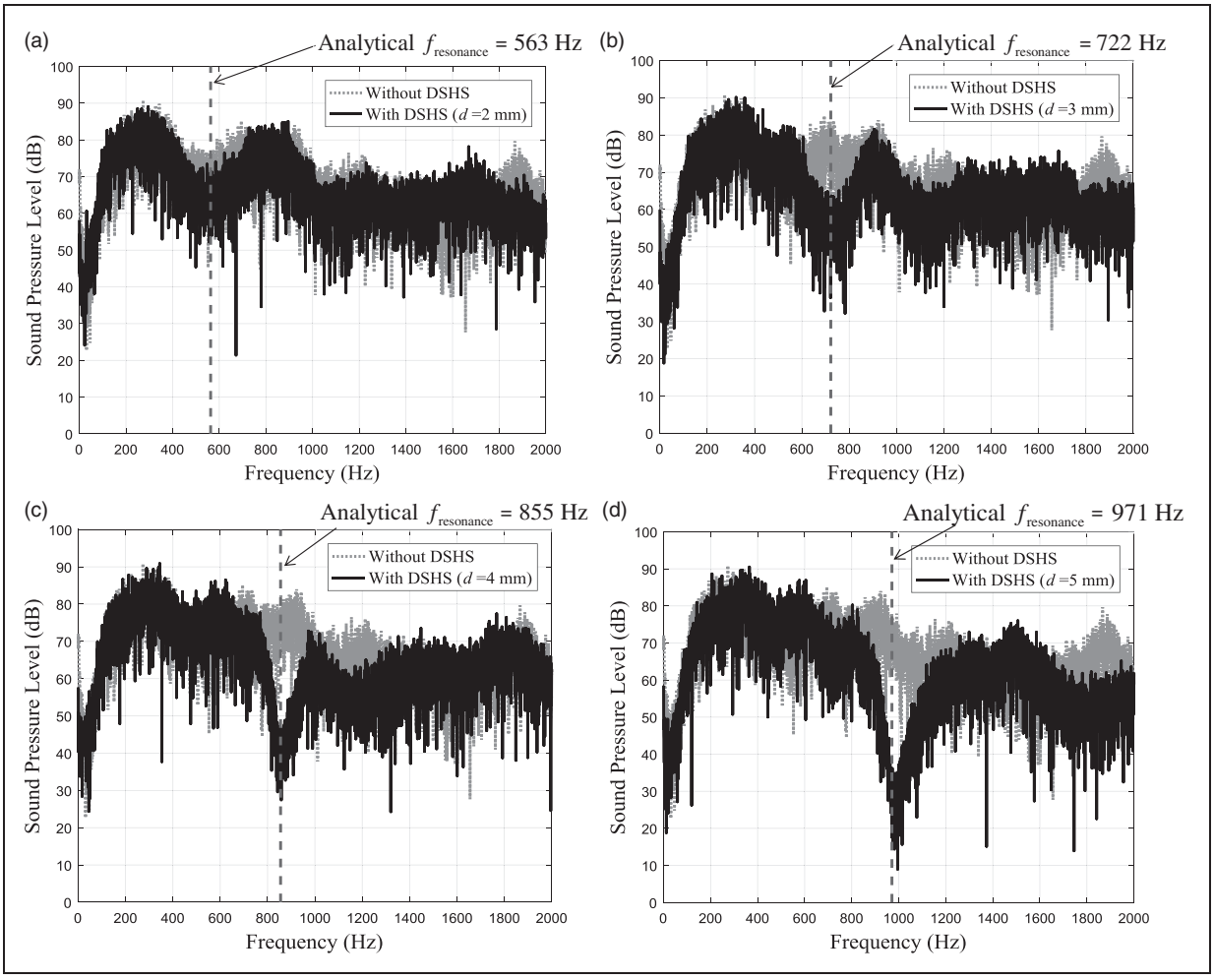

Figure 4. Experimental results for different hole sizes: (a) three double-split hollow sphere (DSHS) structures with 2 mm holes; (b) three DSHS structures with 3 mm holes; (c) three DSHS with 4 mm holes; (d) three DSHS structures with 5 mm holes.

simulated results. It is demonstrated that the resonance frequencies of all DSHS structures in simulation are similar to the theoretical results. As Figure 4 and Figure 5(b) show, the theoretical, simulated, and experimental results are similar to each other.

3. Heterogeneous DSHS and combined heterogeneous DSHS (CHDSHS) structures

3.1. Heterogeneous DSHS structure

In the previous section, DSHS acoustic metamaterial structures with identical side holes were presented (Ding et al., 2013). However, in this study, we allow different sized holes in the acoustic metamaterials, as shown in Figure 6; this structure is termed a HDSHS structure. For this HDSHS structure, the governing equations should be modified as (Kinsler et al., 1999; Blackstock, 2000)

$$\begin{aligned}\text{Time domain}: m_{\text{eff},1}\ddot{x}_1^l &= \frac{S_1\rho_0c^2}{V}\delta V,\ m_{\text{eff},2}\ddot{x}_2^l \\ &= \frac{S_2\rho_0c^2}{V}\delta V \\ \text{Frequency domain}: -\omega^2 m_{\text{eff},1}x_1 &= \frac{S_1\rho_0c^2}{V}\delta V, \\ -\omega^2 m_{\text{eff},2}x_2 &= \frac{S_2\rho_0c^2}{V}\delta V\end{aligned} \tag{5}$$

where δV is the change in volume ($= S_1x_1 + S_2x_2$). The parameters of this model and eigenvalue problem are defined as

$$\begin{aligned}\text{System 1}: k_1 &= \frac{\rho_0c^2S_1^2}{V},\ m_{\text{eff},1} = \rho_0S_1L_1,\ L_1 = t + 1.45d_1/2 \\ \text{System 2}: k_2 &= \frac{\rho_0c^2S_2^2}{V},\ m_{\text{eff},2} = \rho_0S_2L_2,\ L_2 = t + 1.45d_2/2\end{aligned} \tag{6}$$

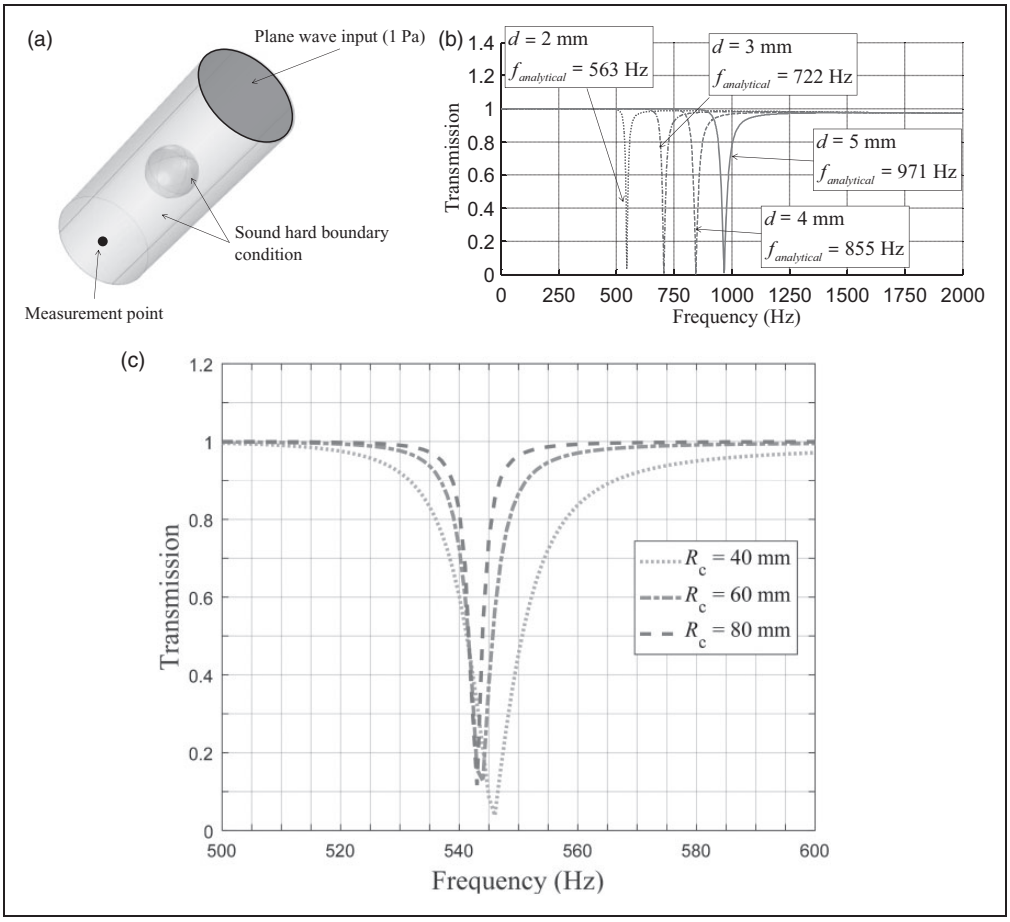

Figure 5. Acoustic impedance finite-element experiment with acoustic duct and DSHS: (a) CAD model and finite-element procedure; (b) transmission curve with respect to various DSHS radii (radius of air duct, 20 mm; thickness of plastic balls, 0.5 mm); (c) transmission curve for different values of R_c (R_c is the radius of the air duct with $f_{resonance} = 563$ Hz at $d = 2$ mm).

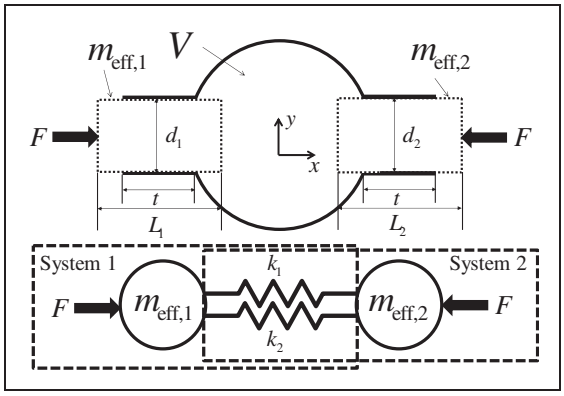

Figure 6. Current HDSHS model and mass–spring model.

$$\det\left(\begin{vmatrix} (k_1 - \omega^2 m_{\text{eff},1}) & \frac{S_2}{S_1}k_1 \\ \frac{S_1}{S_2}k_2 & (k_2 - \omega^2 m_{\text{eff},2}) \end{vmatrix}\right) = 0 \qquad (7)$$

$$f_{\text{resonance}} = \frac{c}{2\pi}\sqrt{\frac{1}{V}\left(\frac{S_1}{L_1} + \frac{S_2}{L_2}\right)} \qquad (8)$$

where the subscript 1 or 2 denotes the quantity corresponding to the structural system, i.e., the diameters of the left and the right necks are set to d_1 and d_2. Without loss of generality, in this study, we consider the following three HDSHS models, HDSHS 1, 2, and 3; their analytical resonance frequencies are computed as 630 Hz, 780 Hz, and 901 Hz from equations (5) to (8).

$$\text{HDSHS } 1 : 2 - 3\text{mm holes}, f_{\text{resonance}} = 630\text{Hz} \qquad (9)$$

$$\text{HDSHS } 2 : 3 - 4\text{mm holes}, f_{\text{resonance}} = 780\text{Hz} \qquad (10)$$

$$\text{HDSHS } 3 : 4 - 5\text{mm holes}, f_{\text{resonance}} = 901\text{Hz} \qquad (11)$$

The involved parameters in equations (5) to (8) can be computed from the values in equations (9) to (11)

when $t = 0.5$ mm, $V = 3.1059 \times 10^{-5}$ mm^3. To test the performance of the HDSHS model numerically, the finite-element model for the acoustic impedance tests was used and the experimental sound pressure levels were measured for the three HDSHS models, as shown in Figure 7. With some differences, their experimental performances agree quite well with our predictions in equations (5) to (8) and (9) to (11).

3.2. Effective properties of HDSHS structures

The resonance frequencies of the HDSHS structures in Figure 7 are 639, 780, and 901 Hz, respectively. The resonant wavelengths are 537, 440, and 381 mm, respectively. It is found that the diameters of the HDSHS structures (= 40 mm) are much smaller than their resonant wavelengths. If the length of the unit cell

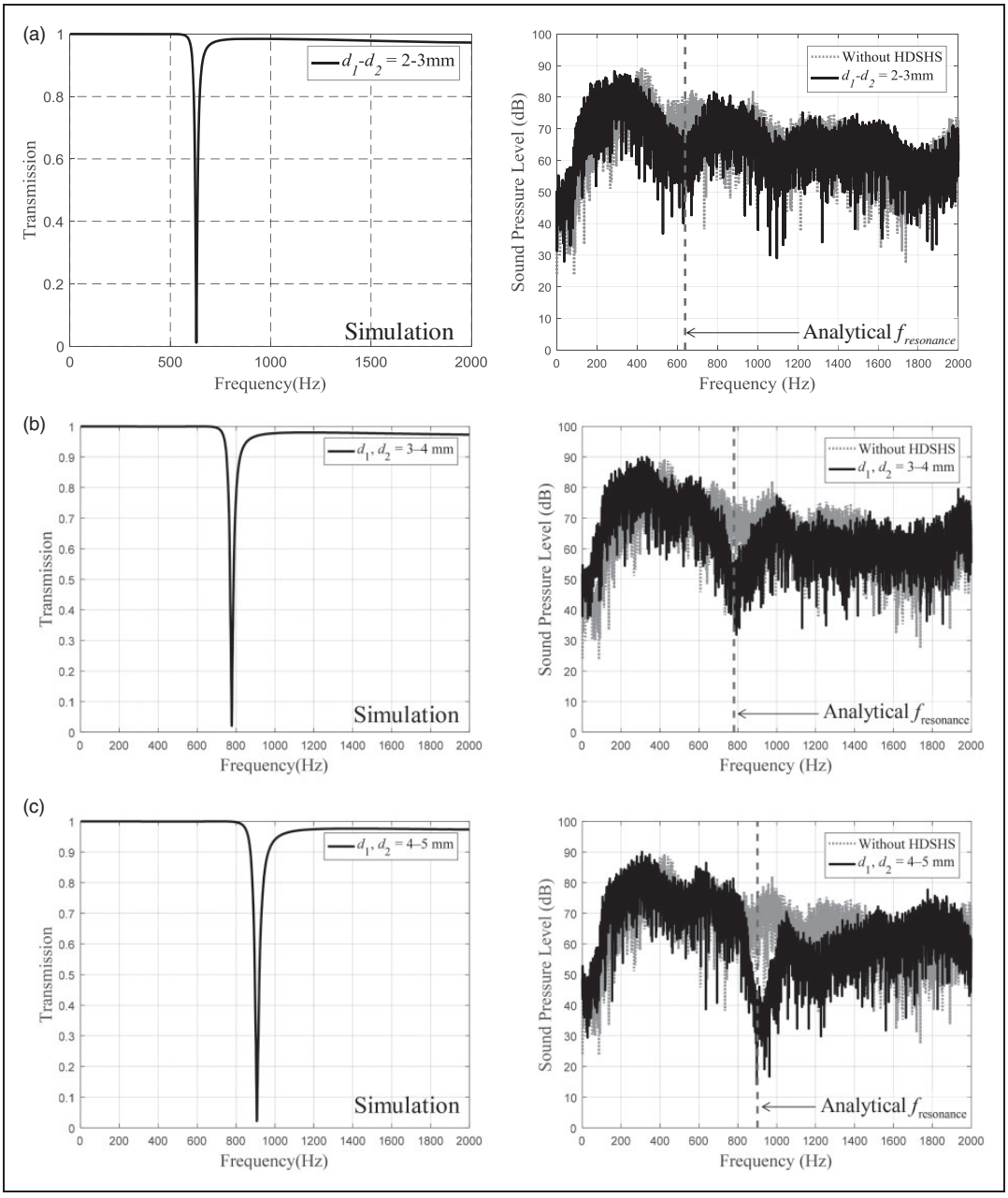

Figure 7. Transmission curves computed by finite-element simulations for the three heterogenous double-split hollow sphere (HDSHS) models and the experimental sound pressure level curves with and without the three HDSHS models. (a) HDSHS 1: 2–3 mm holes, analytical $f_{resonance} = 639$ Hz; (b) HDSHS 2: 3–4 mm holes, analytical $f_{resonance} = 780$ Hz; (c) HDSHS 3: 4–5 mm holes, analytical $f_{resonance} = 901$ Hz.

is much smaller than the wavelength, the acoustic metamaterial can be regarded as a homogeneous material and the method of retrieving effective parameters can be applied. By considering the ratio of the densities ($m = \rho_2/\rho_1$) and the ratio of the speeds of sound ($n = c_1/c_2$) of the acoustic medium and the HDSHS, the reflection (R) and transmission (T) coefficients are formulated as (Fokin et al., 2007; Ding et al., 2013)

$$\text{Reflection coefficient}: R = \frac{\mathrm{i}}{2}\left(\frac{1}{Z_{\text{eff}}} - Z_{\text{eff}}\right)\sin(nkd)T \tag{12}$$

$$\text{Transmission coefficient}: T = \left[\cos(nkd) - \frac{\mathrm{i}}{2}\left(\frac{1}{Z_{\text{eff}}} - Z_{\text{eff}}\right)\sin(nkd)\right]^{-1} \tag{13}$$

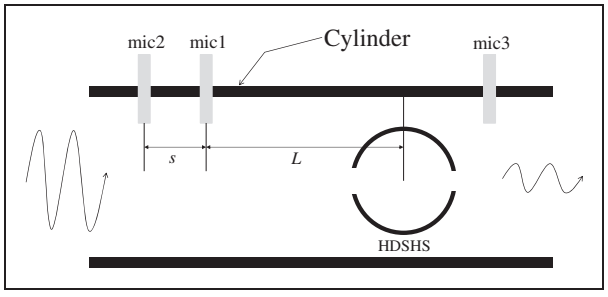

Figure 8. Three-point method of acoustic impedance tube (distance between mic1 and mic2, s; distance between mic1 and center of heterogenous double-split hollow sphere (HDSHS) structure, L; pressure ratio of mic1 and mic2: H_{12}).

where the effective acoustic impedance, the wavenumber, and the thickness of acoustic metamaterial medium are Z_{eff}, k, and d, respectively. The effective acoustic impedance and refractive index based on the retrieving effective parameters can be expressed as

$$Z_{\text{eff}} = \pm\sqrt{\frac{(1+R)^2 - T^2}{(1-R)^2 - T^2}}, \quad n = \frac{1}{kd}\left[2m\pi \pm \cos^{-1}\left(\frac{1-R^2+T^2}{2T}\right)\right] \tag{14}$$

In equation (14), the reflection amplitude can be obtained from the formulation $\left|P_r/P_{\text{in}}\right| = A_r/A_{\text{in}}$, where $P_r = A_r e^{i\varphi}$ and $P_{\text{in}} = A_{\text{in}} e^{i\varphi}$. In our simulation, the three-point method of the impedance tube is illustrated in Figure 8 (Doutres et al., 2010).

The three-point radius is given as

$$R_{3-\text{point}} = \frac{e^{iks} - H_{12}}{H_{12} - e^{-iks}} e^{-2ikL} \tag{15}$$

The acoustic effective bulk modulus (κ_{eff}) of the HDSHS structure is computed as

$$\kappa_{\text{eff}} = \frac{Z_{\text{eff}}\kappa_0}{n} \tag{16}$$

where κ_0 is the impedance of air and ρ_0 is the mass density of air. With these formulations, the computed effective bulk moduli of the HDSHS structures are as shown in Figure 9 and the effective bulk moduli become negative near the resonance frequencies. In previous

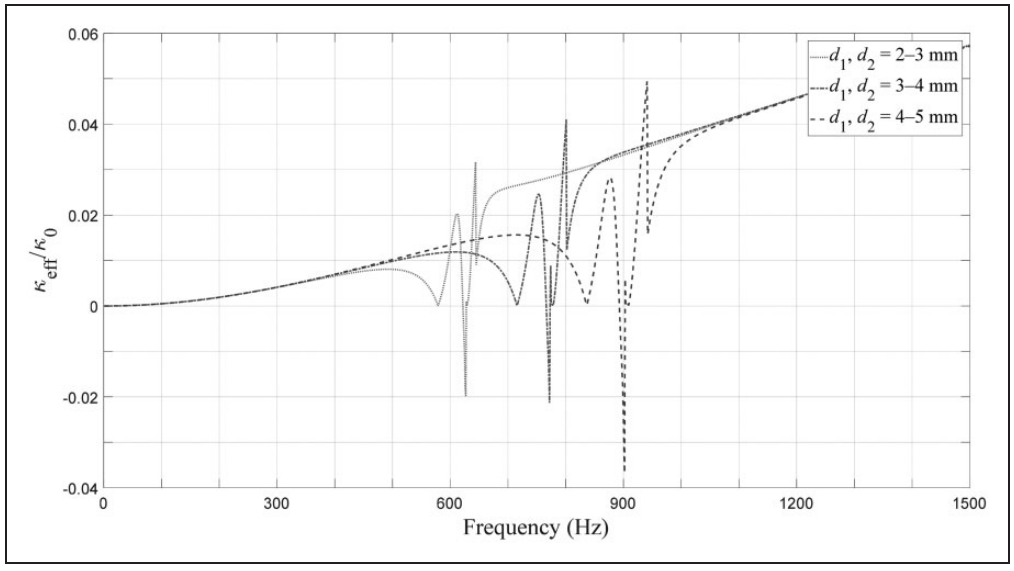

Figure 9. Effective bulk moduli of the present heterogenous double-split hollow sphere structures.

research (Li and Chan, 2004), the effective moduli are repeatedly changed near resonance frequencies. In Figure 9, the effective bulk moduli are changed repeatedly near the resonance frequencies. In summary, the present HDSHS structures show special material properties not found in nature and their dimensions are small, compared with the wavelengths.

3.3. Combined heterogeneous DSHS structure

The present DSHS metamaterial and the present HDSHS metamaterial show significant pressure attenuations at the target frequencies, i.e., approximately 6 dB, compared with the pressure attenuation obtained using a Helmholtz's resonator. However, like other acoustic metamaterials, their stop bands are observed for narrow frequency domains. Some research has been conducted to widen these stop bands by changing the geometrical parameters (Popa and Cummer, 2009; Ding and Zhao, 2011). This study proposes the use of multiple acoustic metamaterials. The combinations of different acoustic metamaterials with different stop bands will increase pressure attenuations over wide frequency ranges. To verify this idea, we consider three

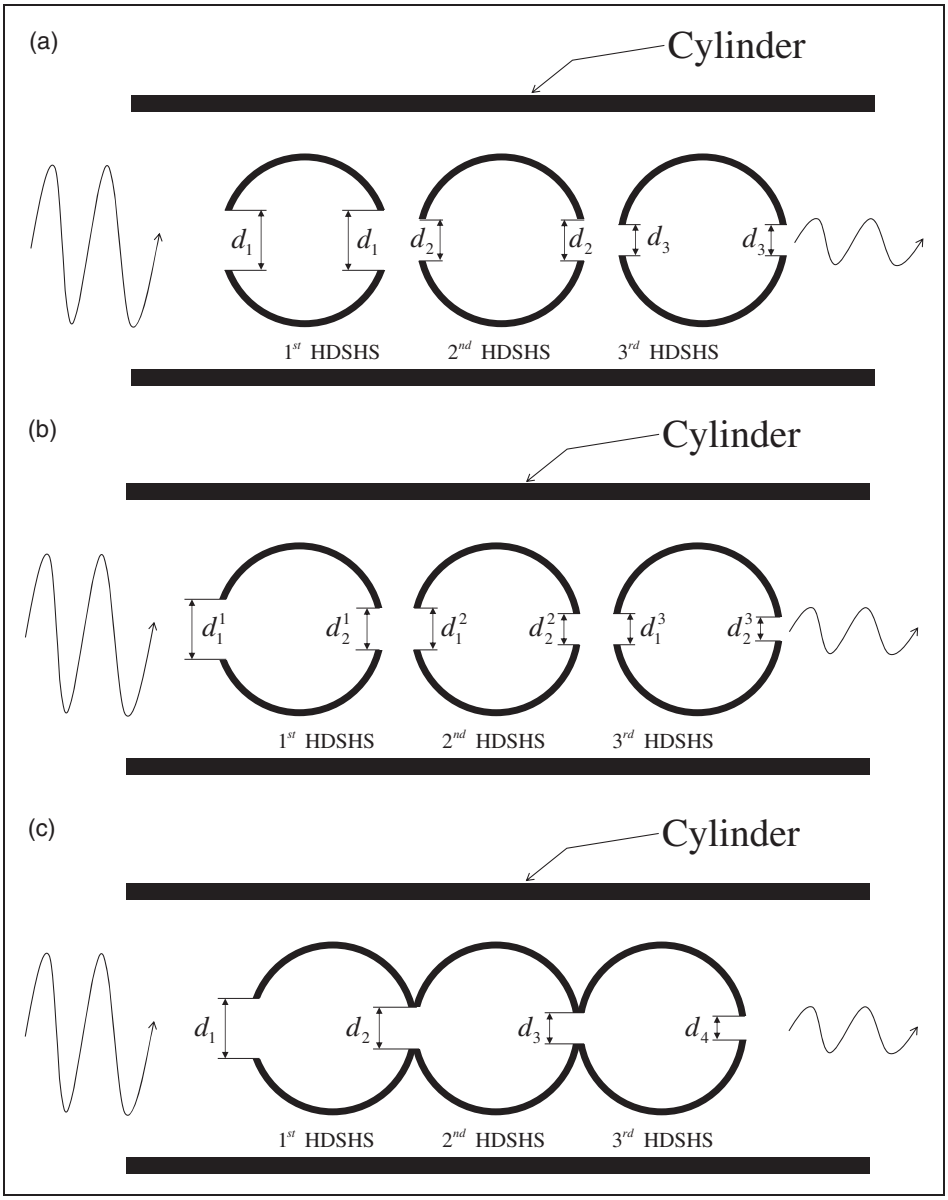

Figure 10. Combined heterogeneous double-split hollow sphere (HDSHS) structures: (a) combined heterogenous double-split hollow sphere (CHDSHS) class 1 model: three separate different double-split hollow sphere (DSHS) structures; (b) CHDSHS class 2 model: three different separate HDSHS structures; (c) CHDSHS class 3 model: combined united HDSHS structure.

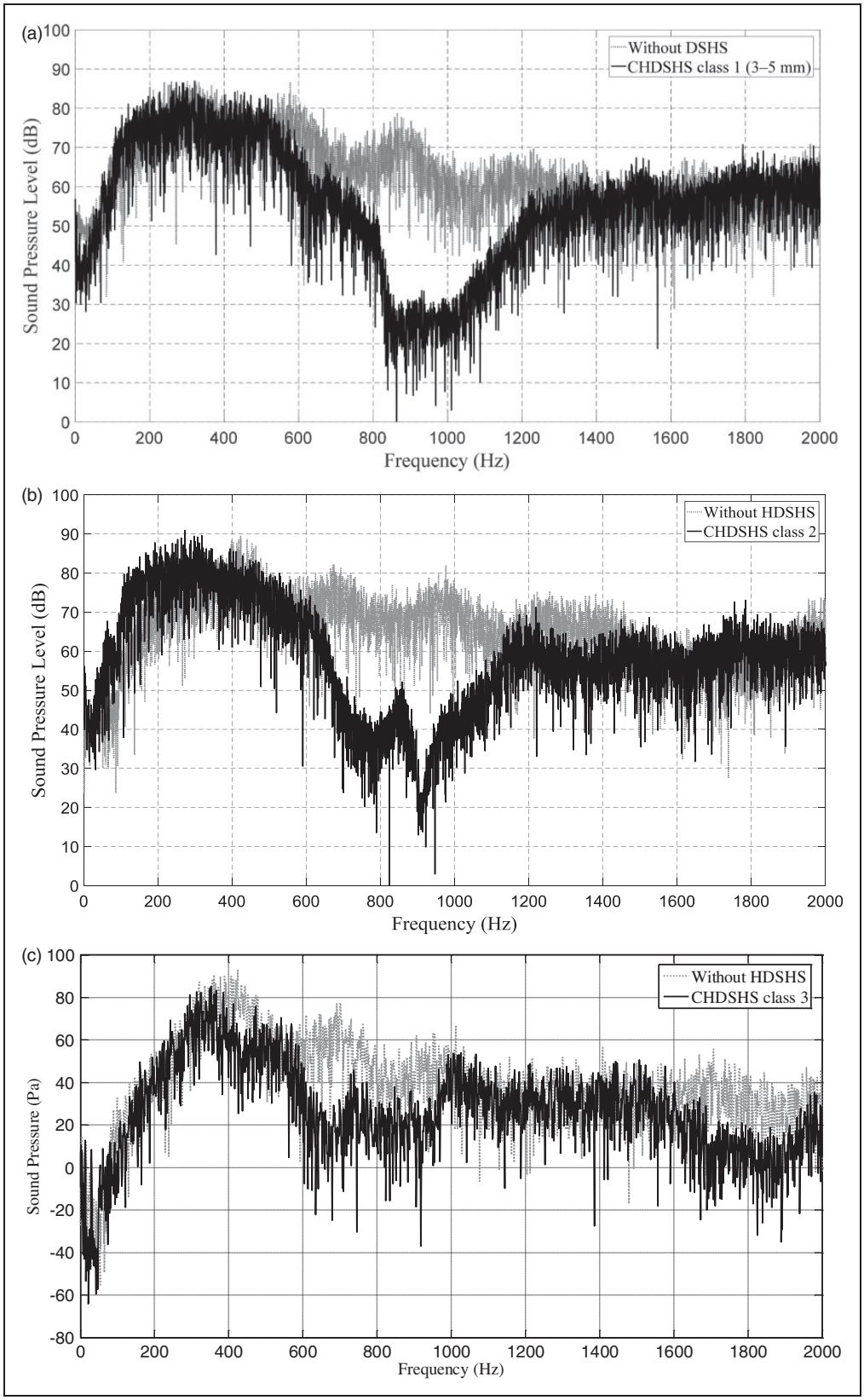

Figure 11. Experimental results of the three combined heterogenous double-split hollow sphere (CHDSHS) models: (a) CHDSHS class 1 model; (b) CHDSHS class 2 model; (c) CHDSHS class 3 model.
DSHS: double-split hollow sphere; HDSHS: heterogeneous double-split hollow sphere.

type combinations, i.e., CHDSHS class 1, CHDSHS class 2, and CHDSHS class 3, as shown in Figure 10. The CHDSHS class 1 model simply combines several different DSHS structures depending on the target stop band ranges. As shown in Figure 10(a), three DSHS structures with 3 mm, 4 mm, and 5 mm holes are located close to each other inside the air duct. The CHDSHS class 2 model combines several HDSHS structures. As shown in Figure 10(b), the model has an arrangement of three HDSHS structures with 2–3 mm, 3–4 mm, and 4–5 mm holes. In the model shown in Figure 10(c), the three HDSHS structures of Figure 10(b) are joined with glue. Note that the HDSHS structures are physically joined for the CHDSHS class 3 model; this can be interpreted as a single structure with multiple resonators. Compared with the CHDSHS class 1 and class 2 models, the performance is inferior because the sum of the areas interacting with the fluid is smaller.

The sound pressure attenuations of the three CHDSHS models were measured experimentally; the results are shown in Figure 11. Comparing with the sound pressure attenuations, the CHDSHS class 1 model, in which the three DSHS structures are arranged separately, significantly reduces the sound pressure from 600 Hz to 1200 Hz. The difference in the acoustic metamaterial shown in Figure 10(c) is that the three metamaterials are joined together. Thus, unlike the separated metamaterials shown in Figure 10(a) and (b), the acoustic energy delivered to the metamaterial shown in Figure 10(c) is relatively uniform. Inside the connected metamaterials, acoustic resonances occur to absorb the acoustic energy inside the metamaterial. Thus, uniform acoustic absorption can be observed in Figure 10(c).

4. Conclusion

To achieve acoustic pressure attenuation over a wide frequency range, this paper presents a new acoustic metamaterial using CHDSHS. For imaging subwavelength features of an object, a metamaterial provides an interesting engineering solution to overcome the diffraction limit in nature by transforming the responsible evanescent waves into propagating waves. Therefore, many numerical and experimental applications can be found. However, the metamaterial also has a limitation because of its narrow operating frequency range. To overcome this limitation and extend the operating frequency range, we propose a combination of several metamaterials. To show this possibility, DSHS structures are considered and the holes of the DSHS structures are varied. The working stop bands of the CHDSHS structures depend on the geometric parameters of the structures. The presented CHDSHS structures show stop bands greater than 600 Hz in experiments. From an engineering point of view, the presented metamaterials can be easily manufactured and installed and the performances of the metamaterials can be accurately theoretically predicted. In our opinion, these characteristics are as important as other acoustic metamaterials, as observed by Ding et al. (2013). It is expected that the presented CHDSHS structures can be applied for the reduction of noise and vibration for various engineering applications.

Declaration of Conflicting Interests

The author(s) declared no potential conflicts of interest with respect to the research, authorship, or publication of this article.

Funding

The author(s) disclosed receipt of the following financial support for the research, authorship, and/or publication of this article: This work was supported by the National Research Foundation of Korea (grant number 2014M3A6B3063711), the Korean Ministry of Science, ICT, and Future Planning, the Human Resources Program in Energy Technology of the Korea Institute of Energy Technology Evaluation and Planning, and the Ministry of Trade, Industry & Energy, Republic of Korea (grant number 20154030200900) and the research fund of Survivability Technology Defense Research Center of Agency for Defense Development of Korea (No. UD150013ID).

References

Airoldi L and Ruzzene M (2011) Design of tunable acoustic metamaterials through periodic arrays of resonant shunted piezos. *New Journal of Physics* 13(11): 113010.

Ambati M, Fang N, Sun C, et al. (2007) Surface resonant states and superlensing in acoustic metamaterials. *Physical Review B* 75(19): 195447.

Blackstock DT (2000) *Fundamentals of Physical Acoustics*. New York, NY: John Wiley & Sons, Inc.

Casadei F, Delpero T, Bergamini A, et al. (2012) Piezoelectric resonator arrays for tunable acoustic waveguides and metamaterials. *Journal of Applied Physics* 112(6): 064902.

Cervera F, Sanchis L, Sanchez-Perez JV, et al. (2002) Refractive acoustic devices for airborne sound. *Physical Review Letters* 88(2): 023902.

Chen S-B, Wen J-H, Wang G, et al. (2011) Locally resonant gaps of phononic beams induced by periodic arrays of resonant shunts. *Chinese Physics Letters* 28(9): 094301.

Chen Y, Huang G, Zhou X, et al. (2014a) Analytical coupled vibroacoustic modeling of membrane-type acoustic metamaterials: Membrane model. *Journal of the Acoustical Society of America* 136(3): 969.

Chen Y, Huang G, Zhou X, et al. (2014b) Analytical coupled vibroacoustic modeling of membrane-type acoustic metamaterials: Plate model. *Journal of the Acoustical Society of America* 136(6): 2926.

Chen YY, Huang GL and Sun CT (2014c) Band gap control in an active elastic metamaterial with negative capacitance

piezoelectric shunting. *Journal of Vibration and Acoustics* 136(6): 061008.
Cheng Y, Xu JY and Liu XJ (2008) One-dimensional structured ultrasonic metamaterials with simultaneously negative dynamic density and modulus. *Physical Review B* 77(4): 045134.
Chiang T-Y, Wu L-Y, Tsai C-N, et al. (2011) A multilayered acoustic hyperlens with acoustic metamaterials. *Applied Physics A* 103(2): 355–359.
Cummer SA and Schurig D (2007) One path to acoustic cloaking. *New Journal of Physics* 9(3): 45–45.
Ding C, Chen H, Zhai S, et al. (2013) Acoustic metamaterial based on multi-split hollow spheres. *Applied Physics A* 112(3): 533–541.
Ding C-L and Zhao X-P (2011) Multi-band and broadband acoustic metamaterial with resonant structures. *Journal of Physics D: Applied Physics* 44(21): 215402.
Ding Y, Liu Z, Qiu C, et al. (2007) Metamaterial with simultaneously negative bulk modulus and mass density. *Physical Review Letters* 99(9): 093904.
Doutres O, Salissou Y, Atalla N, et al. (2010) Evaluation of the acoustic and non-acoustic properties of sound absorbing materials using a three-microphone impedance tube. *Applied Acoustics* 71(6): 506–509.
Fang N, Xi D, Xu J, et al. (2006) Ultrasonic metamaterials with negative modulus. *Nature Materials* 5(6): 452–456.
Fokin V, Ambati M, Sun C, et al. (2007) Method for retrieving effective properties of locally resonant acoustic metamaterials. *Physical Review B* 76(14): 144302.
Guo Z and Sheng M (2016) Bandgap of flexural wave in periodic bi-layer beam. *Journal of Vibration and Control*.
Hirsekorn M (2004) Small-size sonic crystals with strong attenuation bands in the audible frequency range. *Applied Physics Letters* 84(17): 3364.
Huang HH and Sun CT (2009) Wave attenuation mechanism in an acoustic metamaterial with negative effective mass density. *New Journal of Physics* 11(1): 013003.
Huang HH, Sun CT and Huang GL (2009) On the negative effective mass density in acoustic metamaterials. *International Journal of Engineering Science* 47(4): 610–617.
Kinsler LE, Frey AR, Coppens AB, et al. (1999) *Fundamentals of Acoustics*, 4th ed. New York, NY: John Wiley & Sons, Inc., p. 560.
Kshetrimayum RS (2004) A brief intro to metamaterials. *IEEE Potentials* 23(5): 44–46.
Kushwaha MS, Halevi P, Dobrzynski L, et al. (1993) Acoustic band structure of periodic elastic composites. *Physical Review Letters* 71(13): 2022–2025.
Lee HJ, Kim HW and Kim YY (2011) Far-field subwavelength imaging for ultrasonic elastic waves in a plate using an elastic hyperlens. *Applied Physics Letters* 98(24): 241912.
Lee SH, Park CM, Seo YM, et al. (2009) Acoustic metamaterial with negative density. *Physics Letters A* 373(48): 4464–4469.
Li J and Chan CT (2004) Double-negative acoustic metamaterial. *Physical Review. E: Statistical, Nonlinear, and Soft Matter Physics* 70(5 Pt 2): 055602.
Li J, Fok L, Yin X, et al. (2009) Experimental demonstration of an acoustic magnifying hyperlens. *Nature Materials* 8(12): 931–934.
Li J-B, Wang Y-S and Zhang C (2013) Tuning of acoustic bandgaps in phononic crystals with Helmholtz resonators. *Journal of Vibration and Acoustics* 135(3): 031015.
Liu H, Zhao X, Yang Y, et al. (2008) Fabrication of infrared left-handed metamaterials via double template-assisted electrochemical deposition. *Advanced Materials* 20(11): 2050–2054.
Liu Z, Chan CT and Sheng P (2005) Analytic model of phononic crystals with local resonances. *Physical Review B* 71(1): 014103.
Liu Z, Zhang X, Mao Y, et al. (2000) Locally resonant sonic materials. *Science* 289(5485): 1734–1736.
Mead DJ (1970) Free wave propagation in periodically supported, infinite beams. *Journal of Sound and Vibration* 11(2): 181–197.
Pendry JB (2000) Negative refraction makes a perfect lens. *Physical Review Letters* 85(18): 3966.
Pennec Y, Djafari-Rouhani B, Vasseur JO, et al. (2004) Tunable filtering and demultiplexing in phononic crystals with hollow cylinders. *Physical Review. E: Statistical, Nonlinear, and Soft Matter Physics* 69(4 Pt 2): 046608.
Popa B-I and Cummer SA (2009) Design and characterization of broadband acoustic composite metamaterials. *Physical Review B* 80(17): 174303.
Popa BI, Zigoneanu L and Cummer SA (2011) Experimental acoustic ground cloak in air. *Physical Review Letters* 106(25): 253901.
Reynolds M and Daley S (2017) Enhancing the band gap of an active metamaterial. *Journal of Vibration and Control* 23(11): 1782–1791.
Shalaev VM, Cai W, Chettiar UK, et al. (2005) Negative index of refraction in optical metamaterials. *Optics Letters* 30(24): 3356–3358.
Sheng P, Zhang XX, Liu Z, et al. (2003) Locally resonant sonic materials. *Physica B: Condensed Matter* 338(1–4): 201–205.
Smith DR, Pendry JB and Wiltshire MC (2004) Metamaterials and negative refractive index. *Science* 305(5685): 788–792.
Torrent D and Sánchez-Dehesa J (2008) Acoustic cloaking in two dimensions: a feasible approach. *New Journal of Physics* 10(6): 063015.
Wang G, Yu D, Wen J, et al. (2004) One-dimensional phononic crystals with locally resonant structures. *Physics Letters A* 327(5–6): 512–521.
Wang ZG, Lee SH, Kim CK, et al. (2008) Acoustic wave propagation in one-dimensional phononic crystals containing Helmholtz resonators. *Journal of Applied Physics* 103(6): 064907.
Yang Z, Mei J, Yang M, et al. (2008) Membrane-type acoustic metamaterial with negative dynamic mass. *Physical Review Letters* 101(20): 204301.
Yao S, Zhou X and Hu G (2008) Experimental study on negative effective mass in a 1D mass–spring system. *New Journal of Physics* 10(4): 043020.

Zhang S, Yin L and Fang N (2009) Focusing ultrasound with an acoustic metamaterial network. *Physical Review Letters* 102(19): 194301.

Zhang X, Wu D, Sun C, et al. (2007) Artificial phonon–plasmon polariton at the interface of piezoelectric metamaterials and semiconductors. *Physical Review B* 76(8): 085318.

Zhu J, Christensen J, Jung J, et al. (2010) A holey-structured metamaterial for acoustic deep-subwavelength imaging. *Nature Physics* 7(1): 52–55.

Zhu W, Zhao X and Guo J (2008) Multibands of negative refractive indexes in the left-handed metamaterials with multiple dendritic structures. *Applied Physics Letters* 92(24): 241116.